Microchannel Geometries for Improved Heat Transfer with Low-GWP refrigerants

M MUNEESHWARAN*, Cheng-Min YANG, Jamieson BRECHTL, Kashif NAWAZ

Building Technologies Research and Integration Center (BTRIC), Oak Ridge National Laboratory
Oak Ridge, TN 37831, USA

Contact information (muruganm@ornl.gov)

*Corresponding Author

ABSTRACT

Due to efforts aimed at decarbonizing industries, the use of refrigerants with low global warming potential (GWP) is highly recommended in the air-conditioning and refrigeration sectors. Despite possessing low-GWP values of less than 150, hydrofluoroolefins (HFO) exhibit relatively lower heat transfer performance compared to conventional hydrofluorocarbons (HFC) under certain operating conditions. In contrast to HFCs, there is a high demand for enhanced surfaces to meet the needs of heat transfer systems utilizing low GWP refrigerants. Accordingly, this study analyzes the pool boiling performance of low-GWP refrigerants in microchannel geometries. The experiments were carried out at various heat flux levels on both smooth and enhanced surfaces. The pool boiling behavior of low-GWP refrigerant R1234yf was compared to that of R-134a refrigerant in terms of heat transfer coefficient and wall superheat. The results indicate that the heat transfer coefficients of the enhanced surface are significantly higher than those of the smooth surface. Furthermore, the microchannel geometry demonstrated a lower wall superheat compared to the smooth surface. Additionally, a visualization study was performed using a high-speed camera to understand the pool boiling mechanism of low-GWP refrigerants on both smooth and enhanced surfaces.

1. INTRODUCTION

Among all industrial two-phase cooling methods, pool boiling stands out as the most prevalent and mature technique, applicable across both low and high-temperature applications (Liang & Mudawar, 2018). One notable advantage of pool boiling compared to natural or forced convection (without phase change) is its ability to efficiently remove high heat fluxes while maintaining a low wall superheat (Kumar et al., 2023). However, the heat removal capacity of pool boiling is limited by the upper limit of critical heat flux (CHF), which corresponds to a point where the heat transfer coefficient begins to markedly decrease due to the transition from nucleate to film boiling (Mori & Utaka, 2017). This process has been used in multiple thermal energy dissipation systems, including high-power electronics, nuclear reactors, and heat exchangers. Furthermore, pool boiling is the primary mode of heat transfer in flooded evaporators that are employed for air conditioning and refrigeration applications (Lin & Kedzierski, 2019). In high-temperature applications, pool boiling is utilized to rapidly cool alloys from elevated temperatures, facilitating the production of metallic parts with desired microstructural and mechanical properties.

Chlorofluorocarbon (CFC) refrigerants were extensively utilized in the refrigeration and air conditioning sector for several decades. However, their high ozone-depleting potential (ODP) resulted in ozone layer depletion, leading to the initiation of their phase-out in 1986 under the Montreal Protocol. In response, hydrofluorocarbon (HFC) refrigerants, such as HFC134a, were developed as alternatives with significantly lower ODP values (nearly 0). Despite this improvement, the global warming issue has emerged as a major challenge in recent decades. Commonly used HFC134a has a high global warming potential (GWP) of 1430. To address concerns related to high-GWP refrigerants, the Kyoto Protocol of 1997 proposed the elimination of HFC usage. Consequently, global research and development efforts in the refrigeration sector have focused on creating new refrigerants to replace HFC134a, the predominant choice in the current market. As a result of these efforts, hydrofluoroolefins (HFOs) have emerged as promising alternatives to HFCs. Specifically, HFO1234yf has been identified as a potential substitute for HFC134a. Notably,

HFO1234yf boasts a zero ODP and a significantly lower GWP of 4 compared to carbon dioxide, aligning with regulations proposed by the Environmental Protection Agency (EPA) (Park & Jung, 2010).

Numerous studies have reported the pool boiling heat transfer coefficients of R134a for both plain and enhanced surfaces. For instance, Kedzierski (Kedzierski, 2011) and Pialago et al. (Pialago et al., 2013) presented the pool boiling curves of R134a for the plain surfaces. However, being a new refrigerant, pool boiling studies related to R1234yf are limited in the open literature. Several enhanced surfaces have been proposed to augment the pool boiling heat transfer performance, including finned structures, roughened surfaces, and powder-coated (microporous) surfaces. Among these techniques, finned surfaces are more prevalent in the industrial refrigeration sector. Park and Young (Park & Jung, 2010) investigated the pool boiling performance of R1234yf on both plain and low-fin surfaces at a saturation temperature of 7°C and in the heat flux range of 10–200 kW m^{-2}. Their results revealed that the heat transfer coefficients of R1234yf are identical to those of R134a for both the plain and enhanced surfaces. Note that the fin height adapted in their study for the low fin surface is 1.21 mm. Similarly, Ji et al. (Ji et al., 2010) tested the nucleate boiling characteristics of R134a on several finned surfaces with a fin height ranging from 0.56–1.4 mm. Moreno et al. (Moreno et al., 2013) compared the nucleate boiling performance of R1234yf with that of R134a for the saturation temperature range of 20–60°C. Their test results showed that the HTC of R1234yf is similar to that of R134a at lower heat fluxes and it is reduced at higher heat fluxes. Furthermore, the critical heat flux of R1234yf is smaller than that of R134a. Therefore, they proposed microporous surfaces for enhancing the nucleate boiling performance of R1234yf.

In summary, among several enhanced surfaces adapted in the refrigeration industry, finned surfaces are the most prevalent method. The fin heights and widths tested in the open literature are in the millimeter scale, including the common range of 0.5–1.4 mm (Ji et al., 2010). Since micromachining techniques are becoming more viable and affordable, micro-fin surfaces are gaining more attention in pool boiling applications. And the studies available on understanding the pool boiling characteristics of R1234yf on micro-fin structures are scarce in the open literature. Therefore, the goal of this study is to test the nucleate boiling performance of R1234yf on both plain and micro-fin surfaces and compare them with R134a. The pool boiling tests were carried out at a saturation temperature of 15°C and a 25.4 x 25.4 mm^2 surface was used as a heat source.

2. EXPERIMENTAL METHODOLOGY

2.1 Experimental setup

The refrigerant pool boiling setup is mainly composed of a high-pressure vessel, external condenser, chiller loop, pool boiling test section, and data acquisition system, as illustrated in Figure 1(a). The pressure vessel is made of stainless steel. The pressure vessel is equipped with two viewing windows to facilitate visualization of the boiling process. An 800W grounded fiberglass insulated electrical resistance tape heater (BriskHeat CPBIH101016LGT) is wrapped around the outer surface of the vessel to heat up the chamber wall. The desired wall temperature is controlled through a digital PID temperature controller (BriskHeat SDXRA-THRN10-HA). The pressure vessel is fully insulated to reduce heat loss or heat gain from the ambient.

During the pool boiling experiments, the vapor refrigerant rises to the top of the pressure vessel and enters a brazed plate heat exchanger. The plate heat exchanger acts as an external condenser, where the vapor refrigerant is condensed back to liquid phase by exchanging heat with cooling water. The cooling water at a constant temperature is supplied from a 15-kW recirculating chiller (Thermo Scientific, ThermoFlex 15000), and its flow rate is regulated through a control valve to ensure a consistent flow of water at the required temperature to sustain the desired saturation pressure. The system pressure within the vessel is measured using an absolute pressure transducer (Omega PX409-500AI). Two T-type thermocouple probes (Omega TMQSS-062U) are submerged into the liquid refrigerant pool to measure the fluid temperatures at the top and bottom of the vessel. The refrigerants used for the current pool boiling experiments are R134a (GWP=1430) and R1234yf (GWP=4). The related refrigerant properties for these two fluids at a saturation temperature of 15°C are summarized in Table 1.

The heat transfer test section is a T-shaped aluminum heating block designed to boil the liquid refrigerant on top of a flat surface. Two 625W cartridge heaters (Watlow 2257-4887) are installed in the reamed wells at the bottom of the heating block to supply heat. The desired heating power is controlled proportionally through a SCR controller (Watlow DB20-24F0-0000). The power supplied to the cartridge heaters is determined using a watt transducer capable of

measuring within a range of 0 to 500 W (Ohio Semitronics, PC5-107X5Y25). The upper part of the heating block is tapered to a 25.4 mm × 25.4 mm (1 in. × 1 in.) and a 37 mm long neck section, where nine T-type thermocouples (Omega TMQSS-040U) are inserted to measure the temperature gradient. The top surface (25.4 mm × 25.4 mm) of the heating block is acted as a boiling surface. As shown in Figure 1(b), the thermocouple probes are located at a vertical distance of 10 mm from each other, which is subsequently utilized for determining the heat flux. In order to minimize the heat loss, the heating block is wrapped by two-piece PTFE insulation (cover and base). The boiling surface is directly machined on top of the heating block to avoid the issue of contact resistance. In the current study, one smooth surface and one enhanced surface are investigated. The enhanced surface is a tapered micro-fin structure that is directly milled on the test section's top surface. The micro-fin structure is fabricated through end milling process in a CNC machine. It has a series of microgrooves with a fin height of 145 μm, and other dimensional details can be found in Figure 1(c).

2.2 Test Procedure

Prior to the pool boiling experiments, the pressure vessel is evacuated with a vacuum pump for few hours, and then the vacuum condition was left overnight to ensure there is no pressure increase due to the potential leakage of the vessel. Once the system is well checked, the liquid refrigerant is charged into the pressure vessel until it reaches the desired liquid level. The saturation temperature of the refrigerant is maintained by controlling the system pressure through the adjustment of the vessel wall temperature and the inlet temperature and flow rate of the cooling water. When the desired saturation condition is reached, the cartridge heaters are powered to start the pool boiling experiments. The electric power is gradually increased to study the boiling behavior under various heat fluxes.

2.3 Data Reduction

The key parameters for pool boiling performance include the surface heat flux, wall superheat, and the boiling heat transfer coefficient. The surface heat flux is estimated using 1D conduction equation along the upper part of the heating block.

$$q'' = -k\frac{dT}{dx} \tag{1}$$

where k is the thermal conductivity of aluminum and $\frac{dT}{dx}$ is the temperature gradient along the neck of the heating block and it is calculated using the three-point backward Taylor's series approximation. The wall superheat is the temperature difference between the wall and saturation point of the fluid, which is determined by the following equation.

$$\Delta T_{superheat} = T_{wall} - T_{sat} \tag{2}$$

Where T_{sat} is the saturation temperature of the refrigerant under the controlled system pressure and it is determined by the average value of the temperature measurements via the two thermocouple probes submerged in the liquid pool. The wall temperature at the top of the boiling surface T_{wall} is calculated based on the heat flux.

$$T_{wall} = \max\{T_1, T_2, T_3\} - \frac{q''\delta}{k} \tag{3}$$

Where $T1, T2, T3$ is the measured temperature at the center top of the heating block and δ is the distance between the thermocouple probe and the boiling surface.

The pool boiling heat transfer coefficient h for the tested refrigerant is defined as:

$$h = \frac{q''}{\Delta T_{superheat}} \tag{4}$$

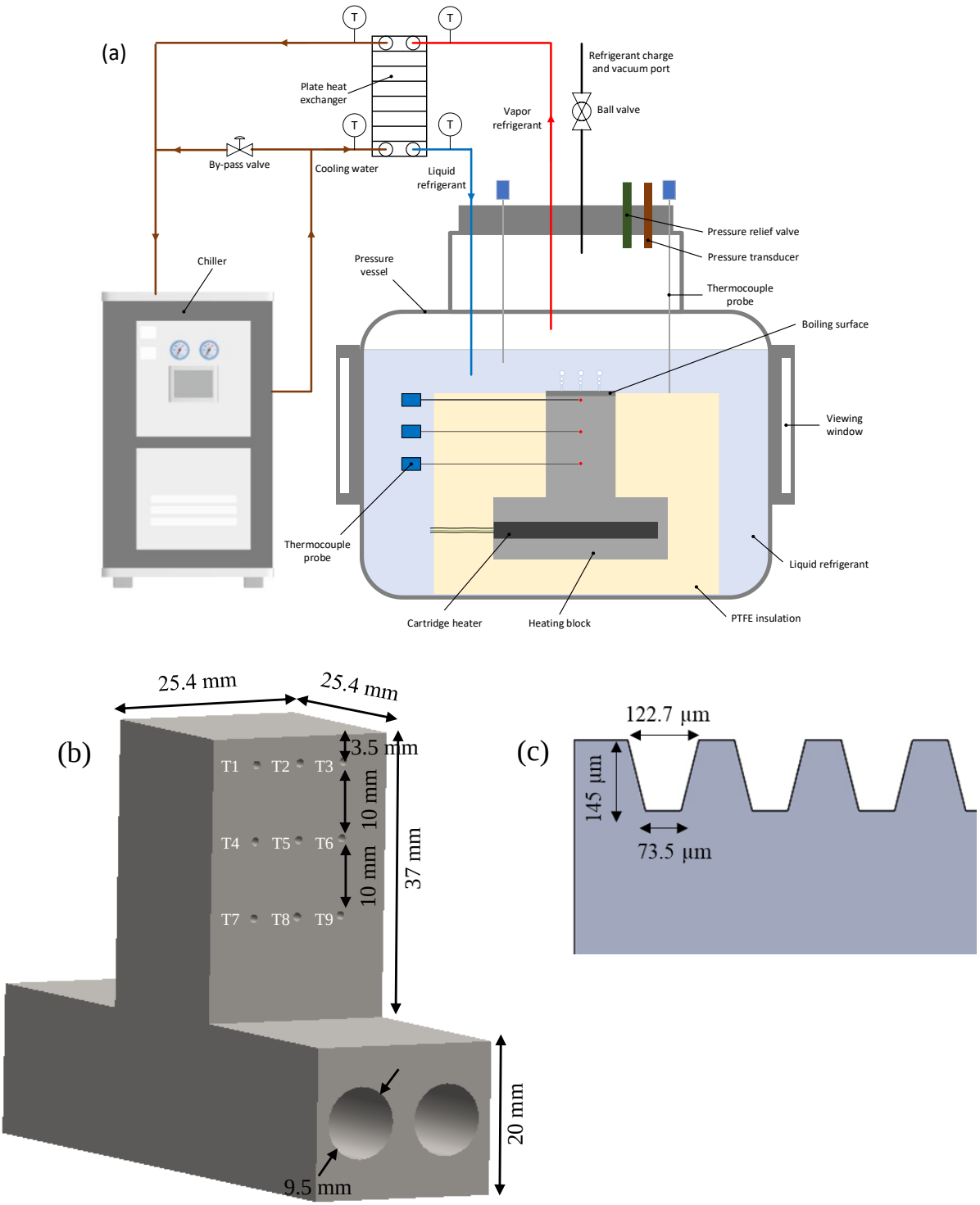

Figure 1: (a) Schematic of the experimental setup, (b) dimensional details of the test section, and (c) dimensional details of the micro-fin structure.

The uncertainties for the above parameters are estimated based on the error propagation methodology reported by Moffat (Moffat, 1988), as shown in Eq. (5).

$$\delta U\left(X_1, X_2, \cdots, X_N\right)=\sqrt{\sum_{i=1}^{N}\left(\frac{\partial U}{\partial X_i}\delta X_i\right)^2} \tag{5}$$

where U is the function of independent variables X_i, and the uncertainties of those independent variables are δX_i, respectively. All uncertainties are reported at a confidence level of 95%. The uncertainty for the heat transfer coefficient is estimated to be within 2%.

3. RESULTS AND DISCUSSION

In this study, the pool boiling characteristics of low-GWP refrigerants within microchannel geometries were investigated and compared against those observed on plain surface results. The heat transfer results of each geometry are discussed in the following sections in terms of heat transfer coefficients and boiling curve. Additionally, visualizations of nucleate boiling phenomenon are presented for both plain and microchannel geometries. Specifically, this study compares the nucleate boiling heat transfer coefficients of R1234yf with those of R134a across both plain and microchannel geometries. The experimental procedures were conducted at a saturation temperature of 15°C and within a heat flux range of 8–200 kW m^{-2}.

The boiling curves for R134a and R1234yf on a plain surface are depicted in Figure 2(a). The boiling curves demonstrate a consistent increase in heat flux with wall superheat, signifying a dominantly nucleate boiling heat transfer mechanism. The nucleate boiling heat transfer coefficients (HTCs) for R134a and R1234yf are plotted against heat flux in Figure 2(b), revealing that the HTCs for both refrigerants rise with increasing heat flux. Notably, Figure 2(b) illustrates that, on a plain surface, the HTCs for R1234yf align closely with those of R134a across the examined heat flux range of 8–200 kW/m². This observation aligns with findings by Moreno et al. (Moreno et al., 2013), who reported identical HTCs for R134a and R1234yf on a plain surface up to a heat flux of approximately 250 kW/m² at a given saturation temperature.

The parity in HTCs between R134a and R1234yf can be attributed to their thermophysical properties and pressure ratios. As mentioned earlier, the experiments were performed at a saturation temperature of 15°C. The saturation pressure, pressure ratio, and other important thermophysical properties of R134a and R1234yf are listed in Table 1. At a saturation temperature of 15°C, the pressure ratio of R1234yf (0.151) is higher than that of R134a (0.12). The pressure ratio is one of the critical conditions in nucleate boiling, which is a ratio of saturation pressure to the critical pressure. The nucleate boiling heat transfer increases with increasing pressure ratio due to the activation of more nucleation sites. Despite having higher pressure ratio, R1234yf exhibited identical HTCs with that of R134a due to its inferior thermophysical properties. For example, latent heat of R1234yf is nearly 18% lower than that of R134a, as listed in Table 1.

In addition to higher pressure ratio, smaller bubble departure diameter also aided R1234yf to match its performance with R134a despite its inferior thermophysical properties. The bubble departure diameter is the maximum size at which a bubble detaches from the boiling surface. The bubble departure diameter (D_d) for R134a and R1234yf is estimated using Fritz relationship (Fritz, 1935):

$$D_d = 0.0208\beta\sqrt{\frac{\sigma}{g\left(\rho_l-\rho_v\right)}} \tag{6}$$

Where $\beta = 35^{\circ}$ for refrigerants, g is the acceleration due to gravity (m s^{-2}), σ represents the surface tension (N m^{-1}), and ρ_l and ρ_v are the liquid and vapor densities (kg m^{-3}), respectively. The bubble departure diameters for R134a and R1234yf, as estimated by the aforementioned model, are 0.644 mm and 0.604 mm, respectively. This indicates that the departure diameter for R1234yf is approximately 6% smaller than that of R134a. This smaller departure diameter, coupled with the higher-pressure ratio, enabled R1234yf to achieve nucleate boiling performance comparable to R134a, despite its inferior thermophysical properties. This aspect of bubble dynamics is critical, as the smaller departure diameter contributes to a more efficient surface renewal during boiling, which compensates for the refrigerant's reduced latent heat and other thermophysical properties drawbacks.

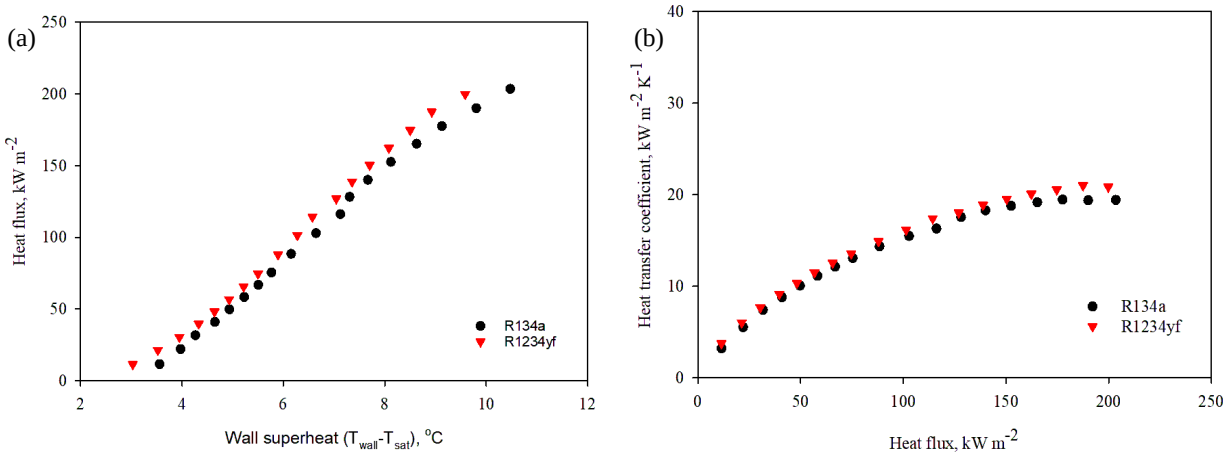

Figure 2. Nucleate boiling heat transfer characteristic of plain surface for R134a and R1234yf (a) boiling curve and (b) heat transfer coefficient.

Table 1: Selected thermophysical properties of R134a and R1234yf at a saturation temperature of 15°C.

Parameters	R134a	R1234yf
Saturation pressure, kPa	488.7	510.2
Pressure ratio	0.12	0.151
Liquid density, kg m^{-3}	1243	1127
Vapor density, kg m^{-3}	23.78	28.26
Latent heat of vaporization, kJ kg^{-1}	186.6	153
Surface tension, mN m^{-1}	9.36	7.44
Dynamic viscosity, mPa s	0.22	0.172
Specific heat, kJ kg^{-1} K^{-1}	1.387	1.347

Similar to observations on a plain surface, the nucleate boiling heat transfer characteristics for microchannel geometries are illustrated in Figure 3. In line with the results from the plain surface, the heat transfer coefficients (HTCs) for both R134a and R1234yf within microchannel geometries are found to be equivalent. However, the heat transfer coefficients of the microchannel geometry are up to 86% higher than that of plain surface. This significant enhancement in HTC can primarily be attributed to the augmented surface area and an increased number of nucleation sites available within microchannel geometries, which collectively contribute to reduced wall superheat. According to Figure 3(a), for the heat flux range of 8–250 kW m^{-2}, the wall superheat is in the range of 3.8°C to 5.3°C, which is significantly lower than that of plain surface. For the same heat flux range, the wall superheat in the plain surface spans from 3.5°C to 10.5°C. The lower wall superheat of microchannel geometry offers nearly 86% increase in HTC than that in plain surface, which is highly preferred in the industrial refrigeration system.

The nucleate boiling behavior on both plain and microchannel geometries was observed using a high-speed camera, with the findings depicted in Figure 4 for a selection of heat flux levels. Initial observations at lower heat fluxes indicate that not all nucleation sites are activated, attributed to the reduced wall superheats at these stages. Under these conditions, bubble growth and detachment processes tend to occur more independently, with a diminished likelihood of bubble coalescence. This phase is characterized by a gradual increase in heat flux alongside wall superheat, predominantly driven by natural convection heat transfer mechanisms. Whereas at high heat fluxes (and at high wall superheats), the nucleation sites are fully activated, and greater number of bubbles have been generated, as shown in Figure 4. Consequently, the frequency of bubbles coalescence phenomenon increases, which in turn, enhances the convective effect. Therefore, the heat flux increases at a faster rate with wall superheat than that in low heat fluxes, as shown in Figures 2 and 3.

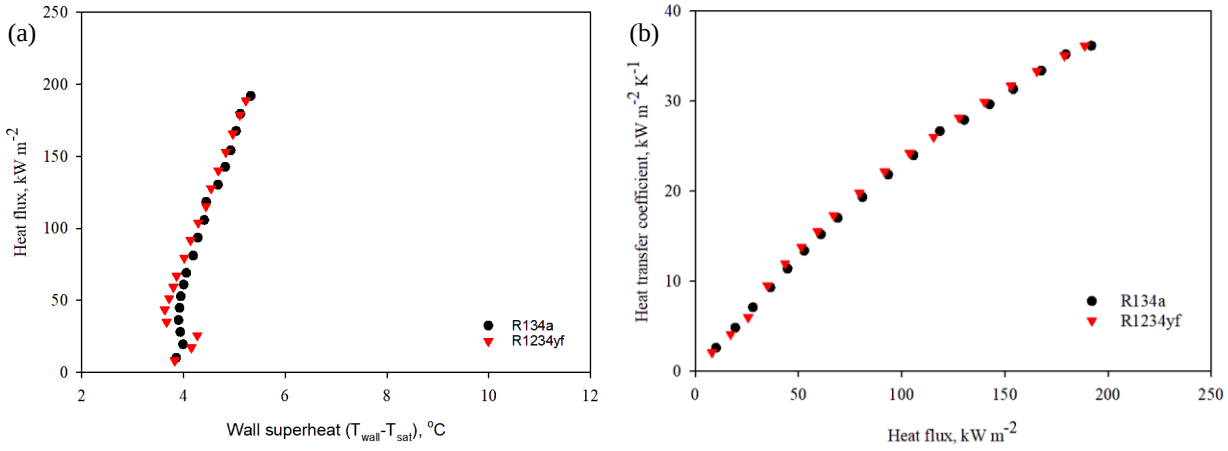

Figure 3. Nucleate boiling heat transfer characteristics of microchannel geometry for R134a and R1234yf (a) boiling curve and (b) heat transfer coefficient.

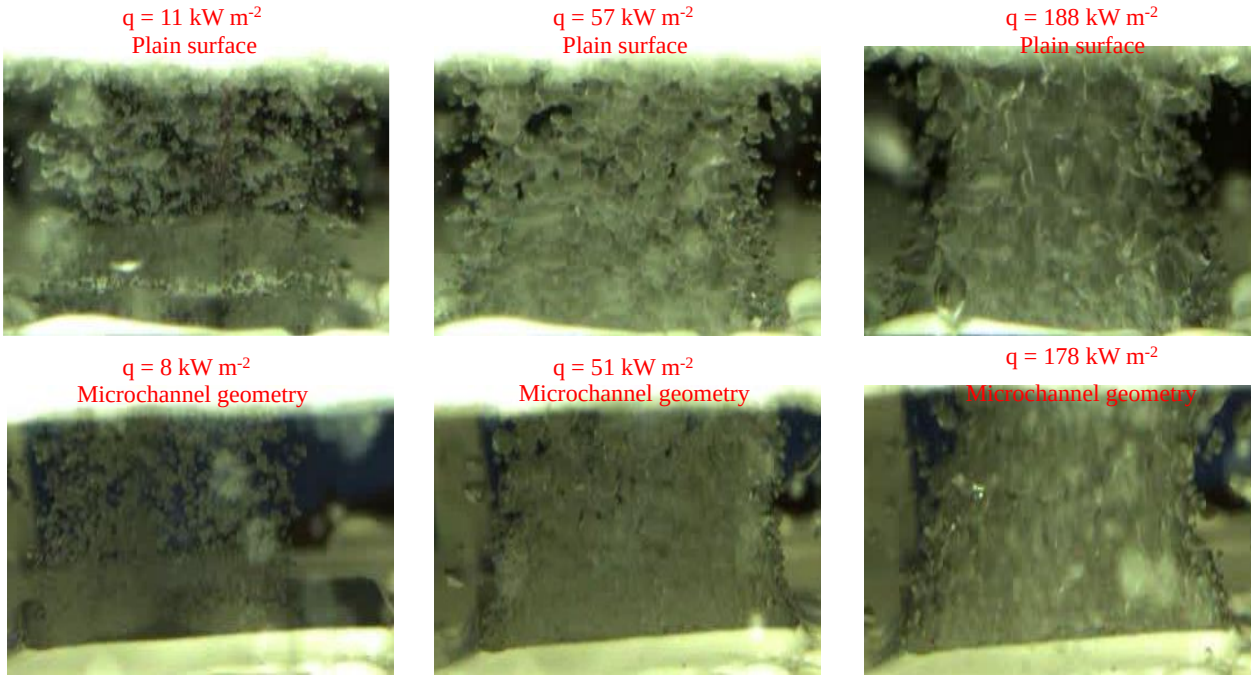

Figure 4. Nucleate boiling behavior of R1234yf on plain and microchannel geometries at different heat fluxes.

4. CONCLUSIONS

In this study, the pool boiling characteristics of R1234yf are studied and compared against R134a. The tests were performed at a saturation temperature of 15ºC and for a heat flux range of 8–200 kW m^{-2}. A novel micro-fin structure has been developed, and its performance has been tested and compared against the plain surface. The following conclusions are drawn based on the experimental findings:

- Heat transfer coefficients of R1234yf on a flat surface are identical to those of R134a for the heat flux range of 8–200 kW m^{-2}.
- The heat transfer coefficients of the proposed novel micro-fin structure are up to 86% higher than those of plain surface.

- For the micro-fin surface, the wall superheat is in the range of 3.8ºC to 5.3ºC for the heat flux range of 8–250 kW m^{-2}, which is significantly lower than that of the plain surface. For the same heat flux range, the wall superheat on the plain surface spans from 3.5ºC to 10.5ºC.

REFERENCES

Fritz, W. (1935). Berechnung des maximalvolumes von dampfblasen. *Physik. Zeitschr*, *36*, 379-384.

Ji, W.-T., Zhang, D.-C., Feng, N., Guo, J.-F., Numata, M., Xi, G., & Tao, W.-Q. (2010). Nucleate pool boiling heat transfer of R134a and R134a-PVE lubricant mixtures on smooth and five enhanced tubes.

Kedzierski, M. A. (2011). Effect of Al2O3 nanolubricant on R134a pool boiling heat transfer. *International journal of refrigeration*, *34*(2), 498-508.

Kumar, A., Muneeshwaran, M., & Wang, C.-C. (2023). Recent progress in pool boiling heat transfer of low GWP refrigerants with the effect of POE lubricant oil. *Thermal Science and Engineering Progress*, 102127.

Liang, G., & Mudawar, I. (2018). Pool boiling critical heat flux (CHF)–Part 1: Review of mechanisms, models, and correlations. *International Journal of Heat and Mass Transfer*, *117*, 1352-1367.

Lin, L., & Kedzierski, M. A. (2019). Review of low-GWP refrigerant pool boiling heat transfer on enhanced surfaces. *International Journal of Heat and Mass Transfer*, *131*, 1279-1303.

Moffat, R. J. (1988). Describing the uncertainties in experimental results. *Experimental Thermal and Fluid Science*, *1*(1), 3-17.

Moreno, G., Narumanchi, S., & King, C. (2013). Pool boiling heat transfer characteristics of HFO-1234yf on plain and microporous-enhanced surfaces. *Journal of Heat Transfer*, *135*(11), 111014.

Mori, S., & Utaka, Y. (2017). Critical heat flux enhancement by surface modification in a saturated pool boiling: A review. *International Journal of Heat and Mass Transfer*, *108*, 2534-2557.

Park, K.-J., & Jung, D. (2010). Nucleate boiling heat transfer coefficients of R1234yf on plain and low fin surfaces. *International journal of refrigeration*, *33*(3), 553-557.

Pialago, E. J. T., Kwon, O. K., & Park, C. W. (2013). Nucleate boiling heat transfer of R134a on cold sprayed CNT–Cu composite coatings. *Applied thermal engineering*, *56*(1-2), 112-119.

ACKNOWLEDEGEMENT

The authors sincerely acknowledge the generous support provided by the U.S. Department of Energy (BTO) and the Building Technologies Research and Integration Center at Oak Ridge National Laboratory. Special gratitude is extended to Dr. Payam Delgoshaei, the HVAC & Refrigeration Technology Manager at the Department of Energy, for his invaluable assistance throughout this project. Additionally, the authors express their appreciation for the technical expertise offered by Anthony Ghel, Brian Goins, Tim Dyer, Chelo Chavez, Charles Pierce, Jeff Taylor, Michael Day, and Douglas Stringfield.